Cathodoluminescence Studies of the Inhomogeneities in Sn-doped Ga_2O_3 Nanowires

S. I. Maximenko, L. Mazeina, Y. N. Picard, J. A. Freitas, Jr., V. M. Bermudez and S. M. Prokes

Electronics Science and Technology Division, US Naval Research Laboratory, 4555 Overlook Avenue, Washington, DC 20375, USA

serguei.maximenko@nrl.navy.mil

Received Date (will be automatically inserted after manuscript is accepted)

ABSTRACT

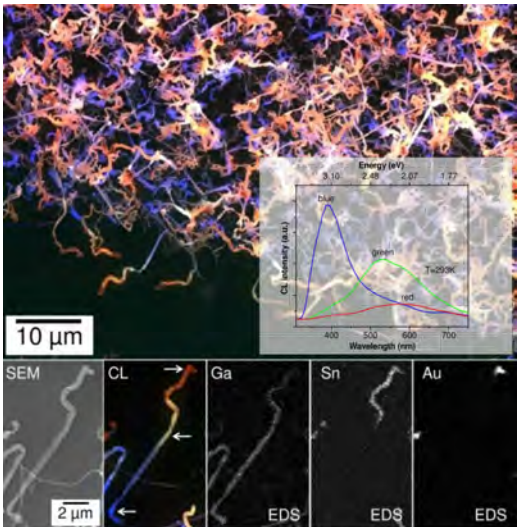

Cathodoluminescence real-color imaging and spectroscopy were employed to study the properties of Ga_2O_3 nanowires grown with different Sn/Ga ratios. The structures grown under Sn-rich conditions show large spectral emission variation, ranging from blue to red, with a green transition zone. Spectral emission changes correlate with changes in the chemical composition and structure found by energy dispersive spectroscopy and electron diffraction. A sharp transition from green to red emission correlates with a phase transition of β-Ga_2O_3 to polycrystalline SnO_2. The origin of the green emission band is discussed based on *ab initio* calculation results.

Recent developments in nanoscience are shifting towards the formation of doped, core-shell nanostructures and heterostructures of semiconductor oxides in order to achieve targeted morphologies, diversity and multi-functionality.[1-8] Non-invasive characterization tools with high spatial resolution are highly desirable in order to study the local structural, optical and electronic properties of the given nanoscale systems. The cathodoluminescence (CL) mode of scanning electron microscope (SEM) has proven to be a powerful tool for probing the local characteristics of low-dimensional materials.[9-10] The spatial resolution of CL is defined primarily by the spherical volume of electron-hole generation created by the electron beam (e-beam) and can be on the order of sub-micron in diameter. It was experimentally demonstrated that 20 nm spatial resolution can be achieved in the CL technique.[11] In some cases, the CL sensitivity is four orders of magnitude better than that of

Report Documentation Page

Form Approved
OMB No. 0704-0188

1. REPORT DATE	2. REPORT TYPE	3. DATES COVERED
2009		**00-00-2009 to 00-00-2009**

4. TITLE AND SUBTITLE	5a. CONTRACT NUMBER
Cathodoluminescence Studies of the Inhomogeneities in Sn-doped Ga2O3 Nanowires	5b. GRANT NUMBER
	5c. PROGRAM ELEMENT NUMBER
6. AUTHOR(S)	5d. PROJECT NUMBER
	5e. TASK NUMBER
	5f. WORK UNIT NUMBER
7. PERFORMING ORGANIZATION NAME(S) AND ADDRESS(ES) **Naval Research Laboratory,Electronics Science and Technology Division,4555 Overlook Avenue SW,Washington,DC,20375**	8. PERFORMING ORGANIZATION REPORT NUMBER
9. SPONSORING/MONITORING AGENCY NAME(S) AND ADDRESS(ES)	10. SPONSOR/MONITOR'S ACRONYM(S)
	11. SPONSOR/MONITOR'S REPORT NUMBER(S)

12. DISTRIBUTION/AVAILABILITY STATEMENT
Approved for public release; distribution unlimited

13. SUPPLEMENTARY NOTES
Nano Letters 9 (2009) 3245

14. ABSTRACT

15. SUBJECT TERMS

16. SECURITY CLASSIFICATION OF:			17. LIMITATION OF ABSTRACT	18. NUMBER OF PAGES	19a. NAME OF RESPONSIBLE PERSON
a. REPORT	b. ABSTRACT	c. THIS PAGE			
unclassified	**unclassified**	**unclassified**	**Same as Report (SAR)**	**7**	

x-ray microanalysis techniques, and impurities with concentrations around 10^{14}·cm^{-3} or lower can be detected.[12] This makes CL a valuable non-destructive tool for studies of inhomogeneities in nanostructures introduced by doping and/or defects. In most cases, CL characterization is limited to simple panchromatic imaging, which does not provide clear information about spectral luminescence variation across the studied specimen. Monochromatic CL imaging and spectroscopy are often implemented in order to obtain this important information. However, monochromatic CL imaging is time consuming and requires multiple scans to obtain comprehensive data that may introduce additional defects due to excessive e-beam radiation.

In this work, real-color CL imaging (RC-CL) and CL spectroscopy were employed to study the properties of undoped (unintentionally doped) β-Ga_2O_3, Sn-doped β-Ga_2O_3 and Ga_2O_3-SnO_2 nanowires (NWs). Sn-doped β-Ga_2O_3 NWs showed uniform luminescence which was red-shifted by 30 nm relative to that of undoped β-Ga_2O_3 NWs. The spectral luminescent variation along the Ga_2O_3-SnO_2 NS was correlated with local structural and chemical properties studied by other SEM-based techniques such as electron backscatter diffraction (EBSD) and energy dispersive spectroscopy (EDS). It is demonstrated that the combination of RC-CL and CL spectroscopy provides a powerful, sensitive, and non-destructive approach to identify inhomogeneities and to study intrinsic and extrinsic properties of nanostructured materials.

The structures studied in the present work were grown at 900 °C by the vapor-liquid-solid (VLS) mechanism under Ar atmosphere as described elsewhere[13] using silicon (100) wafers covered with 20 nm gold films serving as substrates. Undoped β-Ga_2O_3 nanowires were grown using Ga (99.995%)[14,15] while Sn doped β-Ga_2O_3 NWs were grown using 98:2 wt% Ga-Sn alloy (99.999%, Alfa Aesar) as sources.[13] Synthesis of the Ga_2O_3–SnO_2 nanowire heterostructures was performed under the same conditions as described above but using metallic Sn (99.999%, Alfa Aesar) and pure Ga (99.9999%) placed in different zones of the furnace in order to increase the Sn/Ga ratio in the vapor phase.[13]

A conventional LEO 435VP thermal emission SEM equipped with a retractable parabolic collecting mirror was used for the luminescence measurements. A constant-flow liquid helium cold stage was employed to vary the sample temperature in the range between 5 K and 330 K. A probe e-beam with 10 kV accelerating voltage and 1 nA current was used to excite carriers in the target samples for optimal CL signal-to-noise ratio and high spatial resolution. The latter was determined by the size of the electron-hole pair generation sphere and was estimated for our experimental conditions to be ~0.4 µm using the Kanaya and Okayama model.[16] CL imaging was acquired by piping the light emitted by the sample to three fundamental color channels, calibrated to compose real-color CL imaging.[17] The CL spectra were obtained by redirecting the emitted light to a Triax550 spectrometer fitted with a liquid nitrogen cooled CCD camera.[18]

The chemical analysis of the Sn-doped Ga_2O_3 NWs and the Ga_2O_3-SnO_2 heterostructures (HS) was performed by SIMS and EDS. Structural characterization was conducted using a Oxford Instruments Nordlys II EBSD system using a 20 kV, 2.4 nA e-beam. The influence of Sn on the optical properties of Ga_2O_3 was verified by *ab initio* theoretical calculation performed using the procedure described elsewhere.[19]

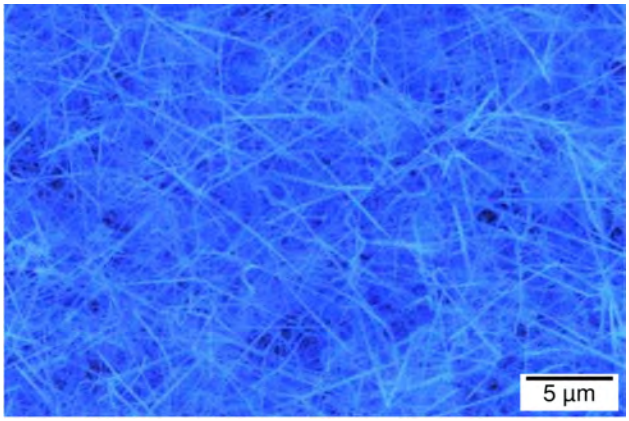

Figure 1. RC-CL image of undoped β-Ga_2O_3 nanowires.

The room-temperature (RT) RC-CL of as-grown undoped monoclinic β-Ga_2O_3 NWs (the crystalline structure identified by TEM, EBSD and FTIR analyses[15]) showed uniform blue emission along the NW lengths (Fig. 1). The emission consisted of a broad asymmetric Gaussian-shaped band with a maximum around 420 nm

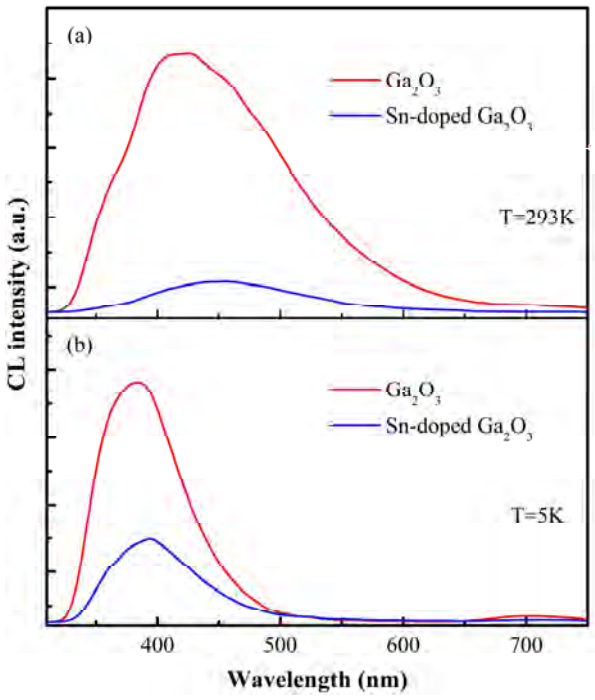

Figure 2. CL spectra of individual undoped and Sn-doped β-Ga_2O_3 NWs measured at (a) 293 K and (b) 5K.

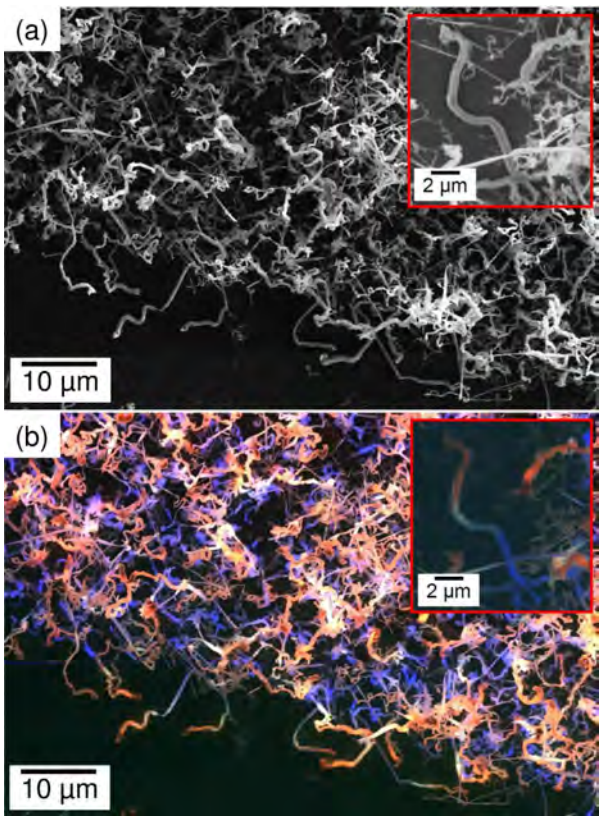

Figure 3. (a) SEM and (b) RC-CL images of Sn-doped Ga_2O_3 NWs grown using the GaSn alloy. Note the color variation along individual wire.

(2.95 eV) and an exponential tail at the lower energy side (Fig. 2). This band becomes narrower and shifts to 380 nm (3.26 eV) at low temperature (~5K). Note that these values are well below the reported near-edge recombination energy value for wide band gap β-Ga_2O_3 (Eg=4.9 eV).[20] The broad blue emission band is a distinctive signature of intrinsic n-type conductivity for bulk and nanocrystaline monoclinic β-Ga_2O_3[21,22] and was assigned to recombination processes between donor-acceptor pair (DAP) centers, where donor and acceptor levels are introduced by oxygen and gallium vacancies, respectively.[21] Characteristic n-type conductivity found in undoped β-Ga_2O_3 has been associated with electrons trapped in oxygen vacancies.[23] The absence of the emission lines at higher energies in the spectra provides evidence that interband emission due to recombination of electron-hole pairs (near bandedge emission) is suppressed by the presence of higher concentration of compensating deep levels. The DAP band is intrinsically broad due to variation of the energy associated with the Columbic interaction between individual donors and acceptors involved in the recombination process. Additional line broadening can be introduced by the large spatial fluctuation in the band edges, due to statistical fluctuation in the local internal fields produced by fluctuations in the density of charged impurities.[24] In addition to the blue band, a low-intensity red emission band was observed at 700 nm (1.77 eV). This band is easily observed in the low temperature CL spectrum (Fig. 2), due to the reduction of the linewidth of emission bands. This band may be related to DAP recombination processes involving electrons trapped by oxygen vacancies and holes captured on deep acceptor levels introduced by nitrogen impurities.[25]

Sn-doped Ga_2O_3 NWs, grown using the GaSn alloy, were formed by the VLS process, where the Sn and Ga from the vapor formed a liquid eutectic droplet with the Au catalyst, leading to a relatively strain and distortion free growth of the monoclinic β-Ga_2O_3 nanowire structure, as confirmed by TEM, EBSD and FTIR analyses.[13] The NWs exhibit morphologies similar to that of pure β-Ga_2O_3 (straight with diameters 100-250 nm and lengths of several microns). This NWs have trace amounts of Sn (0.2 wt%) revealed by chemical analysis of the material. The CL spectra depicted in Fig. 2 showed that the emission peak is red shifted to 450 nm and 390 nm for room and low temperatures, respectively. Similar to undoped Ga_2O_3 NWs (Fig. 1), no emission spectra variations along the length of single NWs or throughout the sample were detected indicating that no Sn segregation occurred. The observed red shift in the emission upon Sn doping correlates with previously reported results, where the introduction of Sn impurity in β-Ga_2O_3 powder promoted a shift of the peak of the emission band from blue to green.[26] Also, it was suggested that the red shift can be attributed to a number of oxygen vacancies presented in the material.[9,27] Despite numerous experimental studies, the recombination mechanism responsible for the green emission is still not understood. Possible mechanisms of the green emission

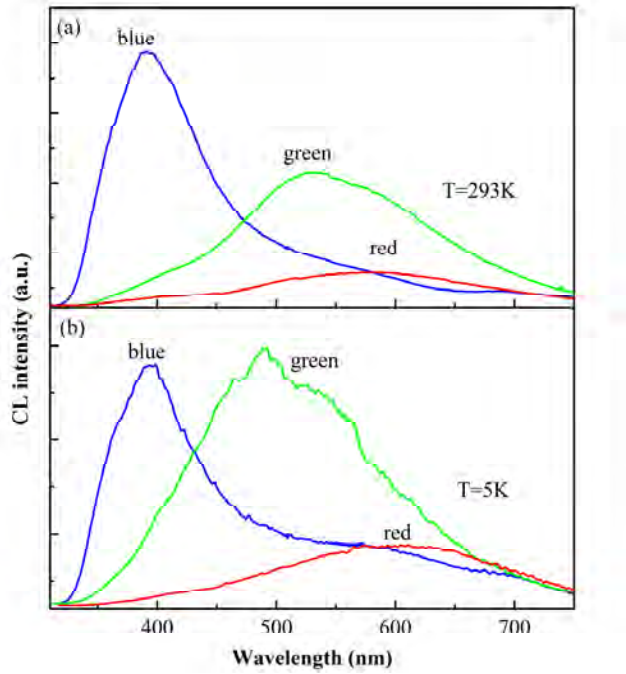

Figure 4. Characteristic CL spectra of blue, green and red emission regions of the nanowires measured at (a) room temperature and (b) at 5K.

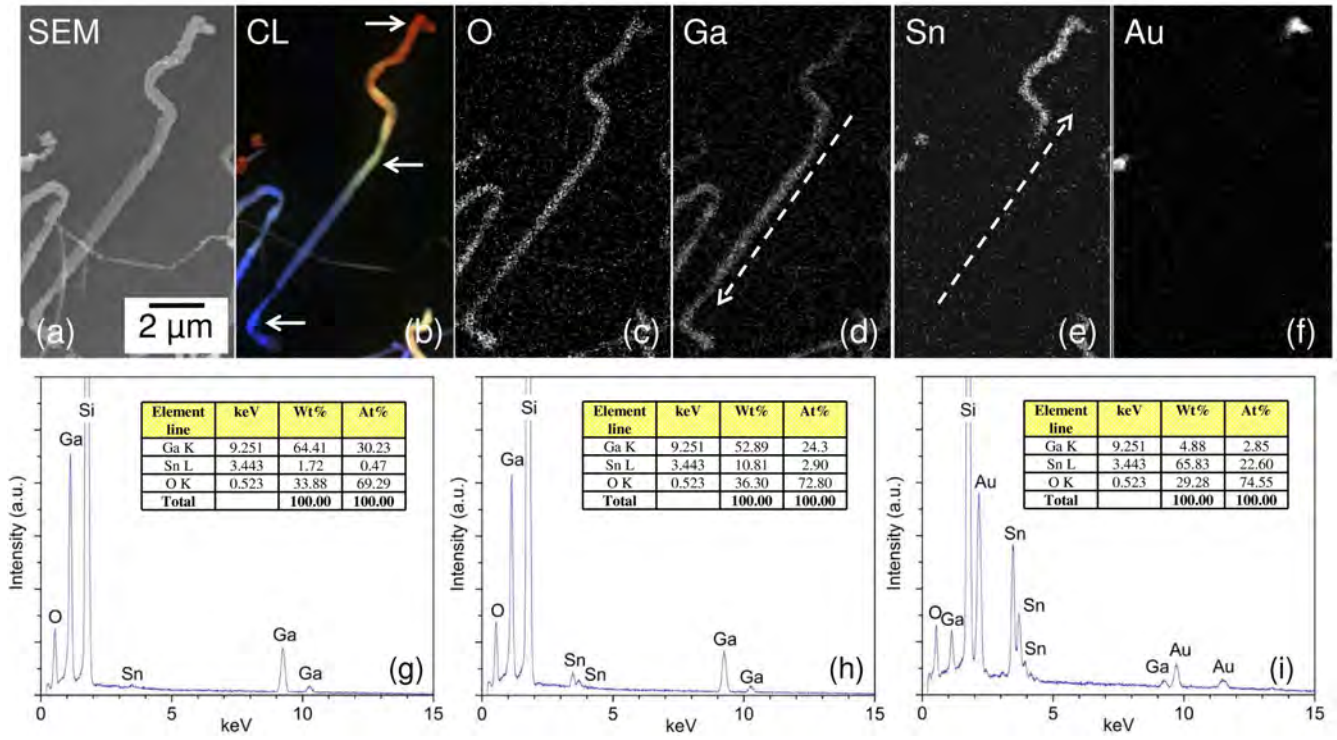

Figure 5. (a) SEM, (b) RC-CLi and EDS analysis of distribution of O (c), Ga (d), Sn (e) and Au (f) acquired from the same nanowire. Arrows on (d) and (e) indicate an increase in the concentration. EDS spectra captured from (g) blue, (h) green and (i) red emission parts of the wire as indicated by arrows in (b). Si signals are generated from the substrate.

will be discussed later in this paper.

RC-CL of NWs grown under Sn-rich conditions revealed that NWs have large spectral emission variations, covering the spectral range from blue to green to red. Note that greater color variations and thickness/shape inhomogeneities are especially pronounced in NWs with larger diameters (500-600 nm) (Fig. 3b) while small diameter NWs (20-100 nm) showed more uniform luminiscence in both straight and kinky parts. High resolution RC-CL of the wires (Fig. 3b, insert) revealed that while the transition from blue to the green emission is gradual, the green to red transition has a noticeable sharp boundary. The red emission is clearly dominant at the top region of the wires, while the regions closer to the Si substrate show increasing blue emission. Room and low temperature CL spectroscopy data acquired in the regions with each individual color emission (blue, green, red) are depicted in Fig. 4. Low temperature CL spectra (Fig. 4b) measured in the blue region of a single NW showed an emission band with a peak around 394 nm (3.15 eV), which corresponds to the peak observed in spectra of Sn doped β-Ga_2O_3 NWs (Fig. 3). The CL spectrum of the "green" region (middle part of the NW) has a peak at around 500 nm (2.48 eV). The CL spectra acquired at the center of the "red"-region has a maximum intensity near 600 nm (2.07 eV).

To identify the mechanisms associated with the large variations in the CL emission spectral distribution, a number of analyses probing the chemical composition and crystalline structure of different parts of NS were carried out. Analysis of the chemical composition by EDS revealed only O, Ga, Sn and Au elements in the wires. Characteristic distribution of the elements and their correlation with RC-CL for one of these nanowires is presented in Fig. 5. The NW region characterized by intense blue emission is rich in Ga with trace amounts of Sn, with Sn content gradually increasing toward the green region to ~1.5-3 wt% (Fig. 5b, d, e). The shift of the spectral peak emission position to lower energy with increased doping concentration is typically associated with bandgap reduction due to heavy doping.[12] The Sn concentration is highest at the top of the NWs, where the red emission dominates (Fig. 5d), while the density of Ga atoms is significantly decreased (down to ~5 wt%). No significant variations in the oxygen content were found along the NW (Fig. 5c). The characteristic signature indicating the VLS growth mechanism is the Au cap observed at the tips of the NWs (Fig. 5f).

The EBSD characterization of the Ga_2O_3-SnO_2 NWs revealed that the parts of the wires with the dominant blue emission have the β-Ga_2O_3 crystalline structure (Fig. 6a). The transition part of the wires with the green emission, which had a high Sn content, was also found to have a β-

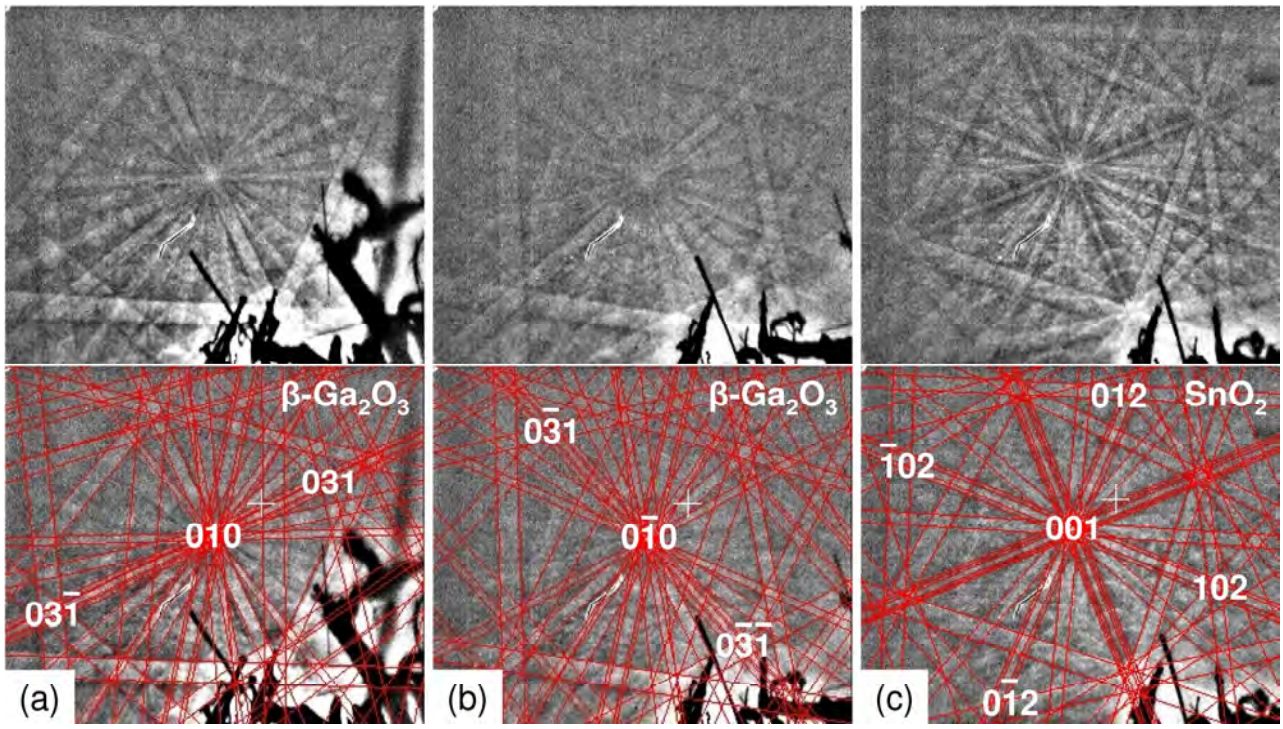

Figure 6. EBSD patterns recorded from (a) blue (b) green and (c) red regions of the Ga_2O_3-SnO_2 nanowires.

Ga_2O_3 crystalline structure (Fig. 6b). However, Kikuchi bands in the recorded EBSD patterns were noticeably weaker, indicating significantly poorer crystalline quality in the green region. The red emission region was identified as rutile-type SnO_2 with numerous variations in orientation, indicating that the SnO_2 was polycrystalline (Fig. 6c). The emission band with peak at ~600 nm (2.07 eV) is consistent with previously reported spectra data for SnO_2.[28] The observed luminescence is probably related to DAP recombination between electrons trapped by oxygen vacancies and holes captured on deep acceptor levels introduced by the Ga impurities. The broad emission band may result from the polycrystalline nature of the wire. It should be mentioned that TEM analysis of the blue-emitting straight parts of the small diameter wires indicated that these regions crystallized as orthorhombic ε-Ga_2O_3.[13] Though no experimental data are available for the band gap value of ε-Ga_2O_3, computational studies showed that this value is close to that of β-Ga_2O_3.[29] The observed blue luminescence band from ε-Ga_2O_3, which correlates with the emission from the low Sn-doped β-Ga_2O_3 sample, probably has the same origin as that of β-Ga_2O_3.

Based on the obtained CL, EBSD and EDS results, we conclude that the factors responsible for the self-assembly of the Ga_2O_3-SnO_2 structures are the different vapor pressures of Sn and Ga as well as different growth kinetics for Ga_2O_3 and SnO_2. First, Ga dissolves in the Au catalyst, resulting in the growth of a well-ordered Sn-doped β-Ga_2O_3 NW. Due to the Ga consumption in the growth, the Ga concentration decreases and at the same time, the relative Sn concentration increases in the vapor phase. Thus, higher amounts of Sn begin to incorporate into the already formed β-Ga_2O_3 structure, inducing strain and distortions that will produce lower crystalline quality β-Ga_2O_3. As more Sn continues to dissolve into the Au catalyst, a polycrystalline SnO_2 phase begins to form which also contains some Ga. Thus, each Ga_2O_3-SnO_2 nanowire consists of three distinct parts: monocrystalline Sn-doped β-Ga_2O_3, poorly crystalline Sn-doped β-Ga_2O_3, and polycrystalline Ga-doped SnO_2. The formation of single ε-Ga_2O_3 NWs during this particular growth process is believed to be related to smaller Au catalyst particles nucleating smaller diameter NWs with larger surface areas, thermodynamically favoring ε-Ga_2O_3 formation over β-Ga_2O_3.[13] Additional studies of these ε-Ga_2O_3 NWs are underway to probe variations in Sn doping concentration.

Rutile tin oxide is an intrinsic n-type direct wide-band-gap (Eg=3.6 eV) semiconductor oxide.[30] The electrical conductivity of tin oxide results primarily from the existence of oxygen vacancies (V_O), which act as donors.[31] However, Ga^{3+} or Ga^{2+} are substitutional impurities, introducing acceptor energy levels within the forbidden gap of SnO_2 and therefore increasing hole concentration.[31] Thus, a transition from n- to p-type conductivity is possible for SnO_2 with an increasing concentration of Ga. This could lead to the formation of n-p heterojunction in a single Ga_2O_3-SnO_2 nanowire.

Based on our observations and previous literature reports,[26] Sn incorporation causes a red shift of the blue

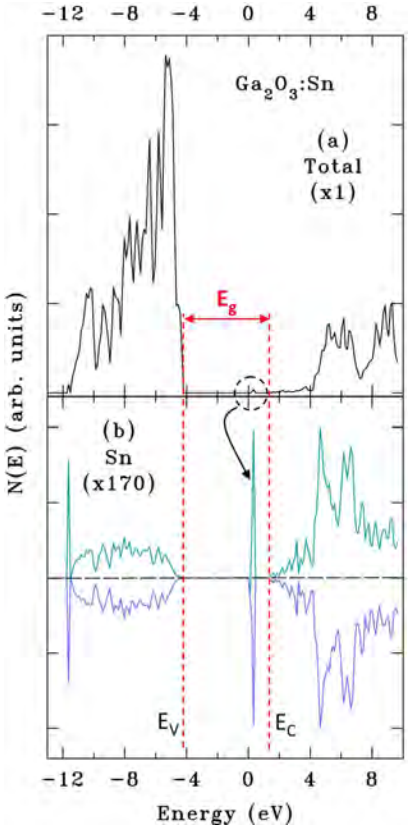

Figure 7. Computed (a) total and (b) Sn projected density of states. The Sn plot shows the virtually identical spin-up and spin-down components. The zero energy is at the Fermi level, and the calculated band gap is Eg= 5.8eV.

emission band in Ga_2O_3. It was suggested that the green emission band may be related to DAP recombination processes, where substituting Ga^{+3} by multivalent Sn results in divalent and tetravalent valence states of Sn which act as donors and as acceptors.[26] However the lack of complete supporting experimental evidence and theoretical studies focused on modeling the energetics of Sn impurity in Ga_2O_3 leave this topic as an open question. In order to verify that a Sn impurity in Ga_2O_3 could be the source of the red-shift in the CL emission band,we performed *ab initio* theoretical calculations. Only the simplest type of defect was considered; namely, a single Sn^{+3} substituting for Ga^{+3}. The model consisted of a periodic lattice built on a supercell of dimensions 1*a* x 4*b* x 2*c*, where *a* = 12.202 Å, *b* = 3.035 Å and *c* = 5.799 Å are the crystallographic unit-cell dimensions of β-Ga_2O_3.[19] The supercell contained 16 Ga_2O_3 units, giving a Sn/Ga ratio of 1/31 or ~3% doping. Previous simulation studies of point defects in Ga_2O_3 using a shell model[32] revealed that in monoclinic β-Ga_2O_3, where Ga atoms occupy both octahedral and tetrahedral sites, Sn^{+4} ions prefer to substitute Ga in octahedral sites. Therefore in our calculations the Sn^{+3} was initially substituted at an octahedral Ga^{+3} site, but this led to severe problems in the convergence of the self-consistent field (SCF) indicating an unstable electronic structure. No such problems were encountered for substitution at a tetrahedral site. The Sn^{+3} involves a single unpaired electron; hence, all calculations were spin-unrestricted. The first step was to relax the geometry to a minimum in the total energy in a Hartree-Fock calculation in which the unit-cell dimensions were fixed but all atoms were free to move. For Ga and O, Durand-Barthelat effective-core pseudopotentials (ECPs) were used with the basis sets optimized for β-Ga_2O_3.[19] Sn was described using the Hay-Wadt large-core ECP with the basis set optimized for SnO_2.[33] After geometry optimization, a single-point density functional theory (DFT) calculation was done using the B3LYP hybrid functional and the all-electron Ga and O basis sets given in Ref. 19 together with the same ECP for Sn. The density of states was then computed using the DFT wavefunction.

The calculation results revealed a Sn-derived state at the Fermi level which lies at about $0.2E_g$ below the conduction band minimum and also a Sn contribution throughout the valence band as presented in Fig. 7. The fully-relaxed electronic configuration of the Sn impurity resembles that of a Sn^{+2} ion. The CL emission can then be interpreted in terms of the recombination of an electron in the Sn-induced gap state with a hole at the top of the valence band. The emission energy of ~3.8eV estimated from this model (using the experimental E_g value of ~4.9 eV) is an upper limit since it neglects any excitonic effect. Although we have not exhaustively studied all possible Sn-related defects, nor analyzed the defect formation energies, the results demonstrate that sub-band-gap emission can reasonably be ascribed to the presence of a Sn impurity. The gradual shift from blue to green emission is probably a result of a competition between intrinsic recombination process involving DAP (donor and acceptor levels introduced by the oxygen and the gallium vacancies) and extrinsic transition from Sn donor level to free holes.

In Figure 8 we present schematically the proposed assignments of various radiative transitions observed in the present work for β-Ga_2O_3 and SnO_2. The recombination channel (a), which is the origin of blue emission, arises from transitions in β-Ga_2O_3 between electron trapped by oxygen vacancies (donor level) and

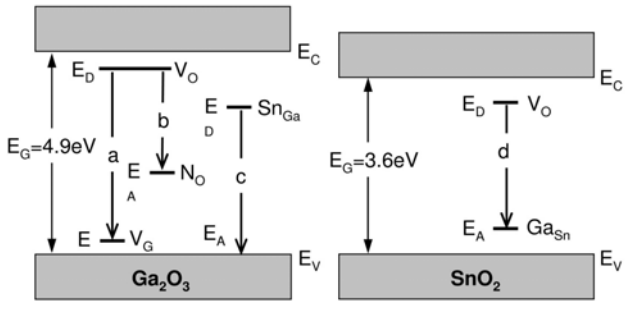

Figure 8. Schematic diagram with the assignments of radiative transitions observed in the studied samples (see text for details).

holes captured by gallium vacancies (acceptor level). The red emission, associated with the recombination channel (b), results from transitions between electrons trapped by theoretical studies focused on modeling the energetics of oxygen vacancies and holes captured on deep acceptor levels introduced by nitrogen impurities. The recombination channel (c) is related to transitions between donor level introduced by the incorporation of Sn atoms in Ga tetrahedral sites of β-Ga_2O_3 and holes at the top of the valence band. The red emission in SnO_2 may result from recombination between the electrons trapped by the oxygen vacancies and holes captured on the deep acceptor levels introduced by Ga impurities, as indicated by recombination channel (d) in Fig. 8.

In summary, we demonstrated the capabilities of SEM-based RC-CL imaging, in combination with point CL spectroscopy, for the detection and identification of local changes of nanostructured material properties. Sn-doped Ga_2O_3 NWs showed uniform luminescence that is 30 nm red-shifted relative to undoped Ga_2O_3 NWs. Ga_2O_3-SnO_2 nanowire heterostructures are characterized by large optical and structural property variations along the length of each individual wire. Three distinct regions characterized by blue, green and red emissions with peak at 390 (3.18 eV), 500 (2.48 eV) and 600 nm (2.07 eV), respectively, were observed. A sharp transition region with emission bands from green to red was observed. EDS and EBSD analyses indicated that these bands are associated with phase transition from Sn-doped monoclinic Ga_2O_3 to Ga-doped rutile SnO_2. A*b initio* calculations demonstrated that the Sn impurity can introduce an energy level in the forbidden gap of β-Ga_2O_3 lying ~0.2 E_g below the conduction band minimum, leading to a donor-to-free-hole transition which is most likely responsible for the spectral red shift of emission band in Sn-doped β-Ga_2O_3 NWs.

Acknowledgment S. I. Maximenko, L. Mazeina and Y. Picard thank the National Research Council (NRC) program for their administrative support. This work was partially supported by the Office of Naval Research (ONR).

(1) Fan, H. J.; Fleischer, F.; Lee, W.; Nielsch, K.; Scholz, R.; Zacharias, M.; Goesele, U.; Dadgar, A.; Krost, A. Superlatt. Microstr. 2004, 36, 95.
(2) Lao, J. Y.; Wen, J. G.; Ren, Z. F. Nano Lett. 2002, 2, 1287.
(3) Gao, P.; Wang, Z. L. J. Phys. Chem. B 2002, 106, 12653.
(4) Kuan, C. Y.; Chou, J. M.; Leu, I. C.; Hon, M. H. J. Sol. St. Chem. 2008, 181, 673.
(5) Zhong, L. W. Mater. Today 2004, 6, 26.
(6) Xu, L.; Su, Y.; Li, S.; Chen, Y.; Zhou, Q.; Yin, S.; Feng, Yi. J. Phys. Chem. B 2007, 111, 760.
(7) Zhang, D.-F.; Sun, L.-D.; Jia, C.-J.; Yan, Z.-G.; You, L.-P.; Yan, C.-H. J. Amer. Chem. Soc. 2005, 127, 13492.
(8) Lugstein, A.; Andrews, A. M.; Steinmair, M.; Hyun, Y.-J.; Bertagnolli, E.; Weil, M.; Pongratz, P.; Schramboeck, M.; Roch, T.; Strasser, G. Nanotechn. 2007, 18, 355306/1.
(9) Yu, D. P.; Bubendorff, J.-L.; Zhou, J. F.; Leprince-Wang, Y.; Troyon, M. Solid State Commun. 2002, 124, 417.
(10) Dovrat, M.; Arad, N.; Zhang, X.-H.; Lee S.-T.; Sa'ar, A. Phys. Rev. B 2007, 75, 205343.
(11) Norman, C. E. Solid State Phenomena 2001, 78-79, 19.
(12) Yacobi, B. G.; Holt, D. B. Cathodoluminescence Microscopy of Inorganic Solids; Springer: Berlin, 1990.
(13) Mazeina, L.; Picard, Y. N.; Maximenko, S. I.; Perkins, F. K., Glaser, E. R., Twigg, M. E; Freitas, J. A; Prokes, S. M. Submitted: Crystal Growth and Design.
(14) Prokes, S. M.; Carlos, W. E.; Glembocki, O. J. Proc. SPIE Intern. Soc. Opt. Enginer. 2005, 6008, 60080C/1.
(15) Mazeina, L.; Picard, Y. N.; Prokes, S. M. Cryst. Growth Design 2009, 9, 1164.
(16) Kanaya, K.; Okayama, S.; J. Phys. D: Appl. Phys. 1972, 5, 43.
(17) Saparin, G. V.; Obyden, S. K. Scanning 1988, 10, 87.
(18) Maximenko, S. I.; Freitas Jr., J. A.; Klein, P. B.; Shrivastava, A.; Sudarshan, T. S. Appl. Phys. Lett. 2009, 94, 092101.
(19) Bermudez, V.M. Chem. Phys. 2006, 323, 193.
(20) Matsumoto, T.; Aoki, M.; Kinoshita, A.; Aono, T. Jpn. J. Appl. Phys. 1974, 13, 1578.
(21) Binet, L.; Gourier, D. J. Phys. Chem. Solids 1998, 59, 1241.
(22) Nogales, E.; Mendez B.; Piqueras, J. Appl. Phys. Lett. 2005, 86, 113112.
(23) Tippins, H.H. Phys. Rev. 1965, 140, A316.
(24) Dean, P.J.; Proc. in Sol. State Chem. 1973, 8, 1126
(25) Song, Y. P.; Zhang, H. Z.; Lin, C.; Zhu, Y. W.; Li, G. H.; Yang, F. H.; and Yu, D. P. Phys. Rev. B 2004, 69, 075304.
(26) Harwing, T.; Kellendonk, F. J. Solid State Chem. 1978, 24, 255.
(27) Villora, E.G.; Atou T.; Sekiguchi, T.; Sugawara, T.; Kikuchi, M.; Fukuda, T.; Solid State Commun. 2001, 120, 455.
(28) De Murcia, M.; Egeet, M.; Fillard, J. P. J. Phys. Chem. Solid. 1978, 39, 629.
(29) Yoshioka, S.; Hayashi, H.; Kuwabara, A.; Oba, F.; Matsunaga, K.;Tanaka, I. J. Phys.: Condens. Matter. 2007, 19, 346211.
(30) Batzill, M.; Diebold, U. Prog. Surf. Sci. 2005, 79, 47.
(31) Bagheri-Mohagheghi, M. –M.; Shokooh-Saremi, M. In Trends in Semiconductor Research; Elliot, T. B., Ed.; Nova: Hauppauge (NY), 2005.
(32) Blanco, M. A.; Sahariah, M. B.; Jiang, H.; Costales, A.; Pandey, R.; Phys. Rev. B 2005, 72, 184103.
(33) Bredow, T.; Pacchioni, G. Theor. Chem. Acc. 2005, 114, 52.